Report on HC 4658

Pressure-induced condensation of organic anhydrides

Experimental

High-pressure experiments were performed using a membrane-driven diamond-anvil cell (DAC).[1] Three experiments were perfomed:

1. Two polymorphs of 2,3-diphenyl maleic acid anhydride (α-DPMA and β-DPMA)
2. Dimethylmaleic dianhydride
3. Maleic anhydride

were placed separately inside the pre-indented steal gaskets (Fig. S1). Subsequently, the DAC was filled with helium as a hydrostatic pressure transmitting medium. Pressure was calibrated using a ruby fluorescence method.[2,3] In situ high-pressure single-crystal synchrotron X-ray diffraction experiments were performed at beamline ID15B at the European Synchrotron Radiation Facility in Grenoble (France). A collimated monochromatic beam (λ = 0.41077 Å) was used. The data collection strategy was a single ω-scan ±32º. The CrysAlisPro software[4] was utilized for collecting diffraction data and their reduction. The crystal structures were solved with program Shelxt[5] and refined by least-squares with Shelxl[6] by using Olex2 software.[7] Structural drawings were prepared using Mercury program.[8] Herein only processed and analysed data for DPMA will be presented. Preliminary studies on maleic anhydride proved an existence of a phase transition (in contrary to literature reports). Dimethylmaeicx anhydride was stable up to 6 GPa, without a phase transition.

Results and discussion

As a result of single-crystal synchrotron X-ray diffraction measurements, the high-pressure crystal structure of α-DPMA and β-DPMA has been determined up to 12.29 GPa. The compressibility plots of α- and β-DPMA are shown in Figure 1. Unit-cell parameters are presented in Table 1 and Table 2.

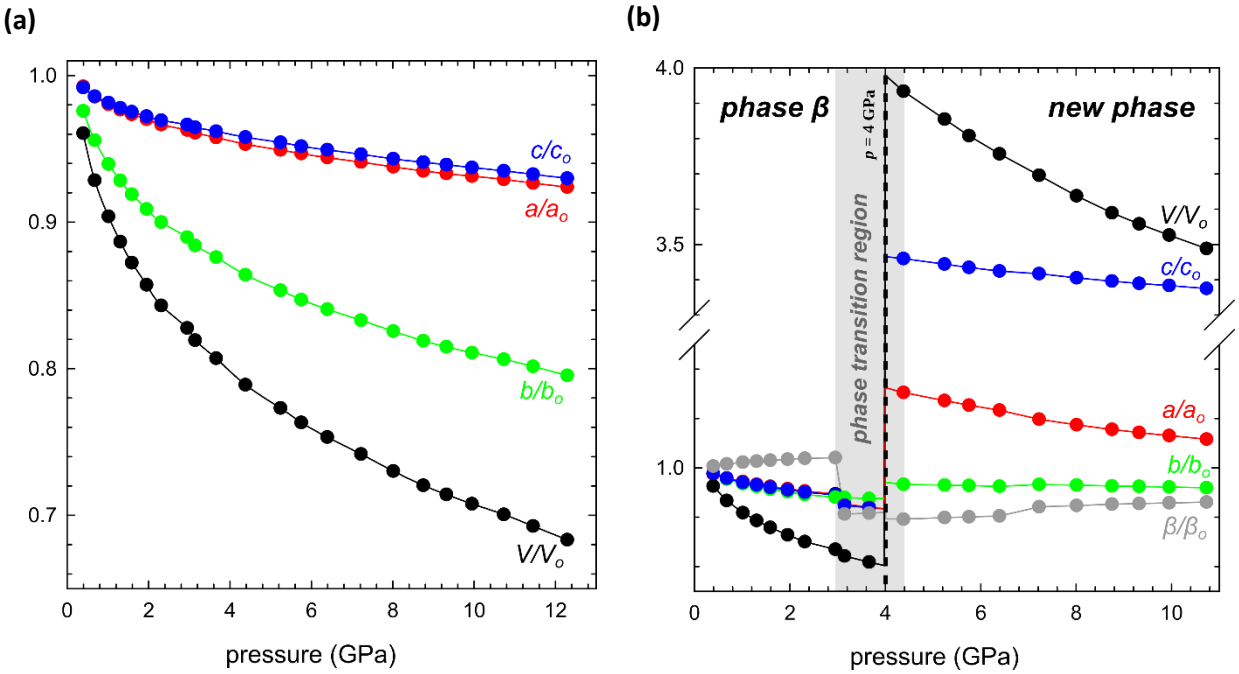

Figure 1. Compression of the unit-cell parameters with increasing pressure for (a) α-DPMA; and (b) β-DPMA, in relation to the average unit-cell dimensions (a_o, b_o, c_o, V_o) at atmospheric pressure. The estimated standard deviations (ESDs) are smaller than the symbols.

Table 1. Selected crystallographic data of α-DPMA with increasing pressure.

pressure (GPa)	*a* (Å)	*b* (Å)	*c* (Å)	*V* (Å^3)	*Z*/*Z*'
0.39	18.8413(19)	13.016(3)	19.5156(19)	4786.1(13)	16/2
0.68	18.7082(13)	12.748(2)	19.3964(13)	4625.8(9)	16/2
1.01	18.6090(14)	12.532(2)	19.3103(13)	4503.2(9)	16/2
1.30	18.5396(12)	12.383(2)	19.2418(12)	4417.4(8)	16/2
1.59	18.4805(13)	12.256(2)	19.1882(12)	4346.1(8)	16/2
1.95	18.4169(10)	12.1227(16)	19.1295(9)	4270.9(6)	16/2
2.31	18.3470(10)	12.0029(17)	19.0756(10)	4200.8(7)	16/2
2.95	18.2778(11)	11.8657(17)	19.0166(10)	4124.3(7)	16/2
3.14	18.2406(9)	11.7915(14)	18.9819(8)	4082.7(6)	16/2
3.66	18.1815(9)	11.6848(15)	18.9273(9)	4021.1(6)	16/2
4.38	18.0953(9)	11.5249(14)	18.8492(8)	3930.9(5)	16/2
5.24	18.0189(10)	11.3833(17)	18.7789(8)	3851.8(6)	16/2
5.75	17.9722(12)	11.2989(14)	18.7274(9)	3802.9(6)	16/2
6.39	17.9207(9)	11.2118(14)	18.6787(8)	3753.0(5)	16/2
7.22	17.8624(9)	11.1108(14)	18.6195(9)	3695.3(5)	16/2
8.01	17.8005(8)	11.0119(13)	18.5584(8)	3637.8(5)	16/2
8.75	17.7483(7)	10.9243(11)	18.5124(7)	3589.3(4)	16/2
9.32	17.7138(8)	10.8699(11)	18.4801(7)	3558.3(4)	16/2
9.95	17.6800(8)	10.8161(10)	18.4417(6)	3526.6(4)	16/2

10.73	17.6398(7)	10.7553(10)	18.3977(7)	3490.4(4)	16/2
11.45	17.5910(7)	10.6903(11)	18.3509(7)	3450.9(4)	16/2
12.29	17.5388(7)	10.6084(10)	18.2975(7)	3404.4(4)	16/2

Table 2. Selected crystallographic data of β-DPMA with increasing pressure.

pressure (GPa)	***a* (Å)**	***b* (Å)**	***c* (Å)**	***β* (°)**	***V* (Å^3)**	**Z/Z'**
0.39	15.042(9)	5.8818(4)	13.7004(11)	101.96(2)	1185.8(7)	4/1
0.68	14.916(6)	5.8175(3)	13.5664(8)	102.405(17)	1149.7(5)	4/1
1.01	14.810(6)	5.7628(3)	13.4467(8)	102.772(16)	1119.3(5)	4/1
1.30	14.724(6)	5.7299(3)	13.3800(8)	102.982(18)	1100.0(5)	4/1
1.59	14.661(5)	5.6974(2)	13.3088(8)	103.181(16)	1082.4(4)	4/1
1.95	14.587(5)	5.6643(2)	13.2382(8)	103.385(16)	1064.1(4)	4/1
2.31	14.521(5)	5.6322(2)	13.1708(8)	103.552(14)	1047.2(3)	4/1
2.95	14.429(5)	5.5996(2)	13.0993(7)	103.725(15)	1028.2(3)	4/1
3.14	14.120(5)	5.5974(3)	12.8042(6)	92.088(12)	1011.3(4)	4/1
3.66	14.020(5)	5.5844(3)	12.7370(8)	92.283(13)	996.4(3)	4/1
4.38	17.562(3)	5.7546(2)	47.943(6)	91.025(14)	4844.3(9)	20/5
5.24	17.3110(15)	5.74710(10)	47.729(4)	91.377(9)	4747.1(6)	20/5
5.75	17.1698(15)	5.74040(10)	47.593(4)	91.530(9)	4689.2(6)	20/5
6.39	17.0129(15)	5.73290(10)	47.452(3)	91.719(8)	4626.1(5)	20/5
7.22	16.7367(18)	5.75420(10)	47.350(4)	93.600(10)	4551.1(6)	20/5
8.01	16.5598(14)	5.74610(10)	47.185(3)	93.865(8)	4479.7(5)	20/5
8.75	16.4195(14)	5.73560(10)	47.060(3)	94.142(8)	4420.4(5)	20/5
9.32	16.3257(14)	5.72990(10)	46.969(3)	94.256(8)	4381.6(5)	20/5
9.95	16.2293(14)	5.72360(10)	46.885(3)	94.397(9)	4342.3(5)	20/5
10.73	16.1208(12)	5.71490(10)	46.772(3)	94.570(7)	4295.4(4)	20/5

As previously reported, the α-polymorph crystallizes in the orthorhombic space group *P*bca with two symmetry independent molecules (Z' = 2).[9] The structure is composed of alternating layers A and B , parallel to the (010) plane (Fig. S2). There are eight A and eight B molecules in the unit cell. For α-DPMA, up to 12.29 GPa, we did not observe a phase transition. The α-DPMA crystal is most compressed along [y], while the compression of the crystal along [x] and [z] are similar (Fig. 1a). This can also be seen in the projections of the unit-cell (Fig. 2); there are free spaces along the b-axis that allow the greatest compression in that direction.

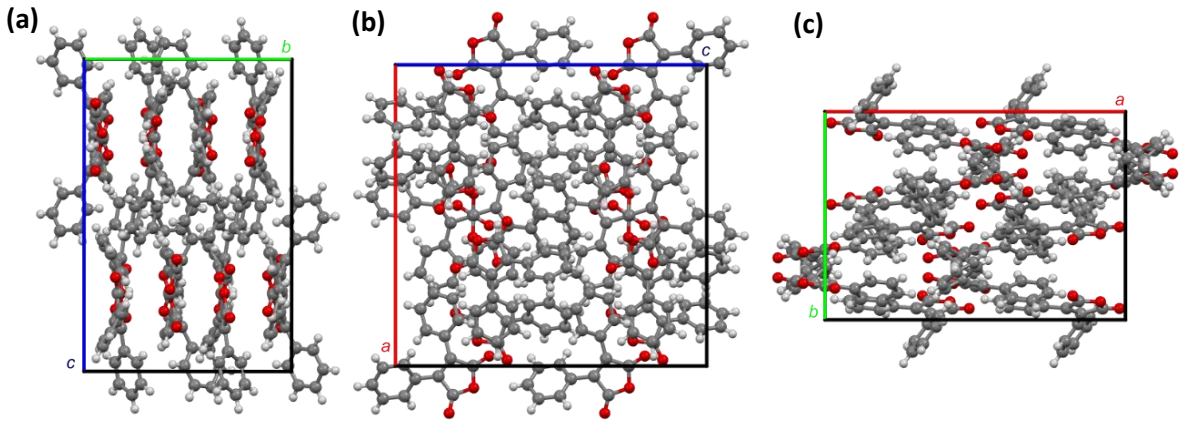

Figure 2. Arrangements of α-DPMA molecules in the unit-cell along direction: (a) [100]; (b) [010]; and (c) [001], at 0.394 GPa.

β-DPMA crystallizes in the monoclinic space group $P2_1/c$ with one symmetry-independent molecule in the unit-cell (Z' = 1). Initially, the compression of the crystal in all three directions is similar. Between 3.70 and 4.35 GPa, it undergoes a phase transition. Interestingly, at approximately 3 GPa we observed a sudden decrease in the β-angle, while the other parameters do not change significantly. This point starts the phase transition region (Fig. 1b). The transition results in a more than 3-fold extension of the c-edge, and an almost 5-fold increase of the unit-cell volume. The number of independent molecules (Z') increases from 1 to 5 (Fig. S3). The space group remains the same, that is $P2_1/c$. Between pressures 6.39 and 7.22 GPa, there is also a significant increase in β-angle with an abnormal b-axis elongation. This is related to the change in the packing of molecules in a unit cell and an increase in topological connectivity. Above 7.22 GPa, the hydrogen bond chains become more branched.

In α-DPMA intermolecular carbonyl-carbonyl (C=O···C=O) interactions are observed, but are not found in β-DPMA (Fig. 3). Previous studies have shown that carbonyl-carbonyl interactions can not only control the geometries of small molecules but also play a significant role in determining the three dimensional structures of proteins, polyesters, and peptides.[10–14] C═O···C═O interaction is characterized by a short O···C distance of less than 3.22 Å (sum of van der Waals radii of carbon and oxygen atoms).[15] As the pressure increases, the CO···CO interactions get stronger, initially more intense and then progressively weaker (Fig. 3b). In α-DPMA, we have identified a structural motif in which one carbonyl group is located above other carbonyl group in an "L- shape" with C=O···C=O dihedral angles (T) close to 90°.[16] There is one-sided interaction where one carbonyl donates and the other carbonyl accepts, only one of the pair of O···C distance is smaller than 3.22 Å (d_1 and d_3).

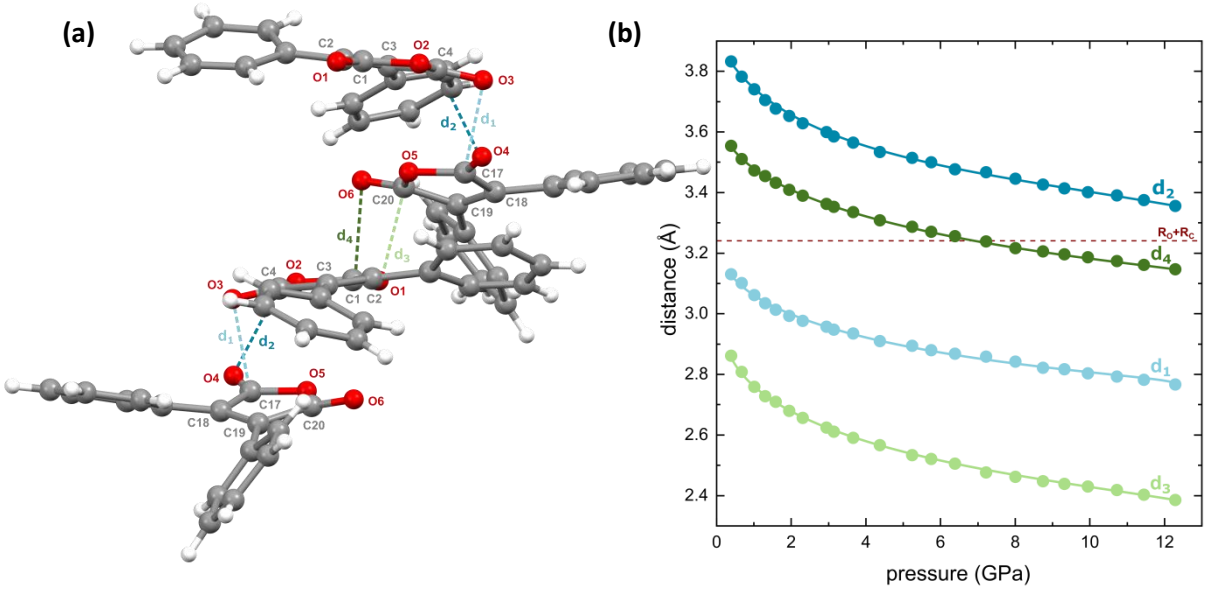

Figure 3. (a) Four α-DPMA molecules with carbonyl-carbonyl (CO···CO) interactions; (b) closest C=O···C=O distances plotted as a function of pressure. The ESDs are smaller than the plotted symbols. The horizontal dashed line indicates the sums of van der Waals radii.[15]

References

(1) Letoullec, R.; Pinceaux, J. P.; Loubeyre, P. The Membrane Diamond Anvil Cell: A New Device For Generating Continuous Pressure And Temperature Variations. *High Press. Res.* **1988**, *1* (1), 77–90. https://doi.org/10.1080/08957958808202482.

(2) Forman, R. A. .; Piermarini, G. J. .; Barnett, J. D.; Block, S. Pressure Measurement Made by the Utilization of Ruby Sharp-Line Luminescence. *Science (80-.).* **1972**, *176* (4032), 284–285.

(3) Piermarini, G. J.; Block, S.; Barnett, J. D.; Forman, R. A. Calibration of the Pressure Dependence of the R1 Ruby Fluorescence Line to 195 Kbar. *J. Appl. Phys.* **1975**, *46* (6), 2774–2780. https://doi.org/10.1063/1.321957.

(4) Rigaku Oxford Diffraction. CrysAlisPro Software System.

(5) Sheldrick, G. M. SHELXT - Integrated Space-Group and Crystal-Structure Determination. *Acta Crystallogr. Sect. A Found. Crystallogr.* **2015**, *71* (1), 3–8. https://doi.org/10.1107/S2053273314026370.

(6) Sheldrick, G. M. Crystal Structure Refinement with SHELXL . *Acta Crystallogr. Sect. C Struct. Chem.* **2015**, *71* (1), 3–8. https://doi.org/10.1107/s2053229614024218.

(7) Dolomanov, O. V.; Bourhis, L. J.; Gildea, R. J.; Howard, J. A. K.; Puschmann, H. OLEX2: A Complete Structure Solution, Refinement and Analysis Program. *J. Appl. Crystallogr.* **2009**, *42* (2), 339–341. https://doi.org/10.1107/S0021889808042726.

(8) Macrae, C. F.; Edgington, P. R.; McCabe, P.; Pidcock, E.; Shields, G. P.; Taylor, R.; Towler, M.; Van De Streek, J. Mercury: Visualization and Analysis of Crystal Structures. *J. Appl. Crystallogr.* **2006**, *39* (3), 453–457. https://doi.org/10.1107/S002188980600731X.

(9) Meents, A.; Kutzke, H.; Jones, M. J.; Wickleder, C.; Klapper, H. Polymorphs of 2 , 3-Diphenyl Maleic Acid Anhydride and 2 , 3-Diphenyl Maleic Imide : Synthesis , Crystal Structures , Lattice Energies and Fluorescence. *Zeitschrift für Krist. - Cryst. Mater.* **2005**, *220* (7), 626–638.

(10) Newberry, R. W.; Raines, R. T. A Key N→π* Interaction in N -Acyl Homoserine Lactones. *ACS Chem. Biol.* **2014**, *9* (4), 880–883. https://doi.org/10.1021/cb500022u.

(11) Newberry, R. W.; Bartlett, G. J.; VanVeller, B.; Woolfson, D. N.; Raines, R. T. Signatures of N→π* Interactions in Proteins. *Protein Sci.* **2014**, *23* (3), 284–288. https://doi.org/10.1002/pro.2413.

(12) Bolton, W. The Crystal Structure of Triketoindane (Anhydrous Ninhydrin). A Structure Showing Close C O ... C Interactions. *Acta Crystallogr.* **1965**, *18* (1), 5–10. https://doi.org/10.1107/s0365110x65000026.

(13) Bartlett, G. J.; Newberry, R. W.; Vanveller, B.; Raines, R. T.; Woolfson, D. N. Interplay of Hydrogen Bonds and n →π* Interactions in Proteins. *J. Am. Chem. Soc.* **2013**, *135* (49), 18682–18688. https://doi.org/10.1021/ja4106122.

(14) Rahim, A.; Saha, P.; Jha, K. K.; Sukumar, N.; Sarma, B. K. Reciprocal Carbonyl-Carbonyl Interactions

in Small Molecules and Proteins. *Nat. Commun.* **2017**, *8* (1), 1–12. https://doi.org/10.1038/s41467-017-00081-x.

(15) Bondi, A. Van Der Waals Volumes and Radii. *J. Phys. Chem.* **1964**, *68* (3), 441–451. https://doi.org/10.1021/j100785a001.

(16) Sahariah, B.; Sarma, B. K. Relative Orientation of the Carbonyl Groups Determines the Nature of Orbital Interactions in Carbonyl-Carbonyl Short Contacts. *Chem. Sci.* **2019**, *10* (3), 909–917. https://doi.org/10.1039/c8sc04221g.

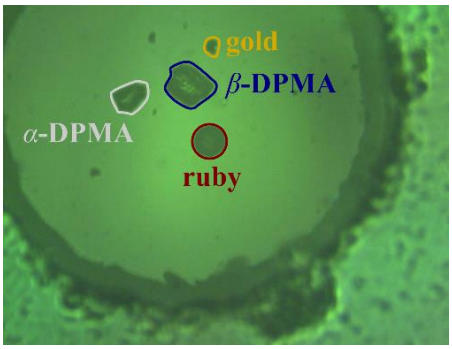

Figure S1. DAC chamber during measurement at 0.394 GPa.

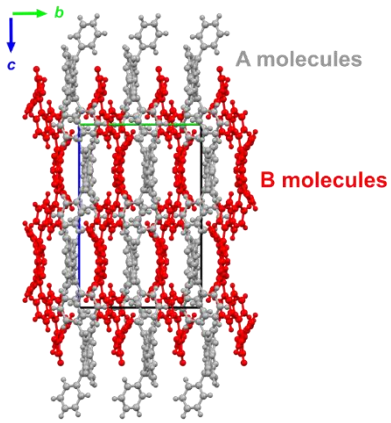

Figure S2. Arrangement of alternating layers of molecules A and B in the α-DPMA crystal in the direction [100].

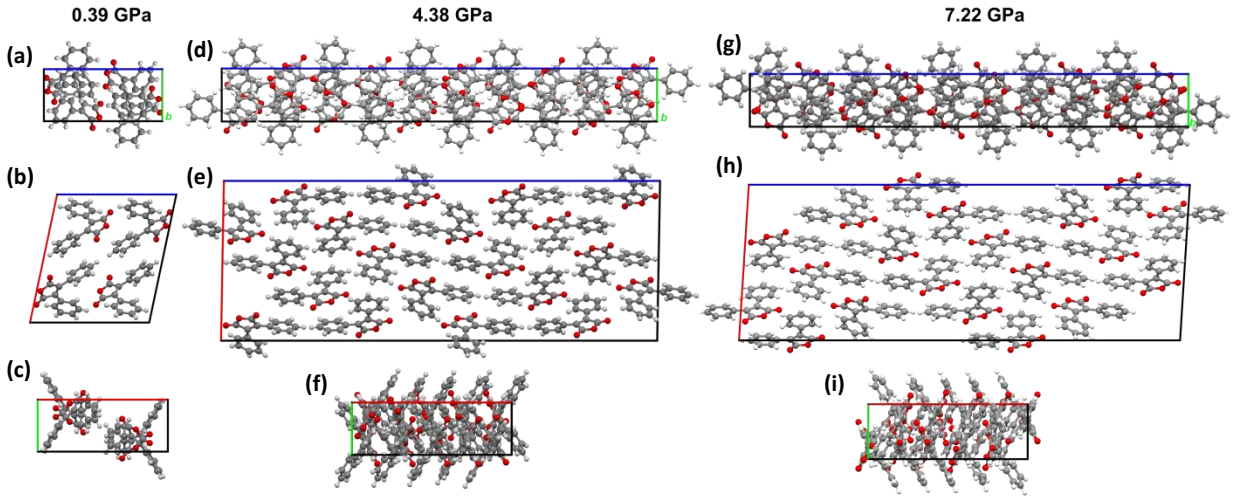

Figure S3. Arrangements of β-DPMA molecules in the unit-cell at 0.394 GPa along direction: (a) [100]; (b) [001]; and (c) [001]; at 4.38 GPa along: (d) [100]; (e) [010]; and (f) [001] and at 7.22 GPa along (g) [100]; (h) [010]; and (i) [001].

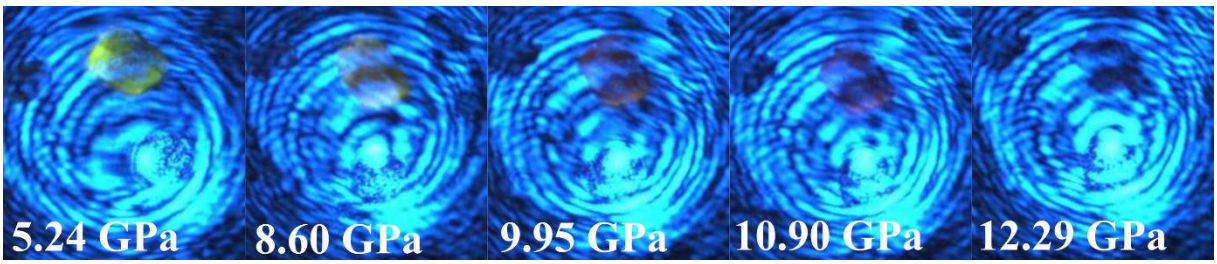

Figure S4. β-DPMA in DAC chamber during the pressure measurements.

Table S1. Compressibility related to crystallographic axes calculated for α-DPMA with Birch-Murnaghan Coefficients in range between 0.394 GPa – 12.29 GPa.

Axes	K(TPa^{-1})	σK(TPa^{-1})	Direction			Empirical parameters			
			a	b	c	ε_0	λ	P_c	v
X_1	11.4072	0.0646	0.0000	-1.0000	0.0000	1.9448e-01	-2.2679e-01	-0.0853	0.2046
X_2	4.5252	0.0205	-1.0000	0.0000	0.0000	1.8227e-02	-3.2488e-02	0.1572	0.3948
X_3	4.2038	0.0203	0.0000	0.0000	1.0000	5.2632e-03	-1.9316e-02	0.3200	0.5038
V	23.3844	2.0035							

Birch-Murnaghan Coefficients

	B_0 (GPa)	σB_0 (GPa)	V_0 (Å^3)	σV_0 (Å^3)	B'	σB'	P_c (GPa)
2nd	20.0738	0.8492	4660.0064	31.0035	4	n/a	0
3rd	6.7744	0.9413	4957.6126	41.4243	10.1028	0.9582	0

Table S2. Compressibility related to crystallographic axes calculated for β-DPMA with Birch-Murnaghan Coefficients in range between 0.394 GPa - 3.659 GPa.

Axes	K(TPa^{-1})	σK(TPa^{-1})	Direction			Empirical parameters			
			a	b	c	ε_0	λ	P_c	v
X_1	47.7825	10.5210	0.6256	0.0000	0.7802	-7.9386e-03	-1.5379e-02	0.3940	1.8214
X_2	10.5029	0.5754	0.0000	-1.0000	0.0000	1.2888e+01	-1.2908e+01	-0.0410	0.0019
X_3	-9.0328	13.5714	0.7421	0.0000	-0.6703	-1.7238e-02	1.5261e-04	0.3940	4.8480
V	47.9033	4.1015							

Birch-Murnaghan Coefficients

	B_0 (GPa)	σB_0 (GPa)	V_0 (Å^3)	σV_0 (Å^3)	B'	σB'	P_c (GPa)

2nd	12.8585	0.7222	1204.1769	7.1979	4	n/a	0
3rd	5.9240	3.0486	1243.1825	27.7639	10.7501	5.0601	0

Table S3. Compressibility related to crystallographic axes calculated for a new phase of *β*-DPMA with Birch-Murnaghan Coefficients in range between 4.38 GPa – 10.73 GPa.

Axes	***K*(TPa^{-1})**	**σ*K*(TPa^{-1})**	**Direction**			**Empirical parameters**			
			a	***b***	***c***	ε_0	λ	P_c	ν
X_1	13.4378	1.2935	-0.9850	0.0000	-0.1723	6.4282e+00	-6.2300e+00	-0.5672	0.0193
X_2	1.5880	0.8209	0.7860	0.0000	-0.6183	1.0291e-02	-1.2781e-06	-24.003	2.7520
X_3	1.1345	0.9193	0.0000	1.0000	0.0000	-1.6164e-03	-3.6831e-06	4.3800	3.9534
V	18.0251	0.7245							

Birch-Murnaghan Coefficients

	***B*$_0$ (GPa)**	**σ*B*$_0$ (GPa)**	***V*$_0$ (Å^3)**	**σ*V*$_0$ (Å^3)**	***B*'**	**σ*B*'**	***P*$_c$ (GPa)**
2nd	56.8636	14.0598	4971.6105	107.4852	4	n/a	0
3rd	7.8839	6.4860	6049.8427	358.0922	9.1464	4.5192	0